# An overview of the three-color simultaneous imager HinOTORI telescope

**Wei Liu,[a,b*] Yousuke Utsumi,[c,d,e] Koji Kawabata,[f] Yongqiang Yao,[g] Mahito Sasada,[f] Hiroki Nagashima,[f] Zheng Lou,[a] Zhiping Jin,[a] Bin Li,[a] Tianrui Sun,[a] Yingxi Zuo,[a] ShengCai Shi[a]**

[a] Purple Mountain Observatory, Chinese Academy of Sciences, Nanjing, China, 210033
[b] University of Chinese Academy of Sciences, Beijing, China
[c] Kavli Institute for Particle Astrophysics and Cosmology, Menlo Park, California, United States
[d] SLAC National Accelerator Laboratory, Menlo Park, California, United States
[e] Stanford University, Menlo Park, California, United States
[f] Hiroshima Astrophysical Science Center, Hiroshima University, Hiroshima, Japan
[g] National Astronomical Observatories of China, Chinese Academy of Sciences, Beijing, China

**Abstract:** HinOTORI is a China-Japanese international cooperation 50cm telescope to observe the Gravitational Waves (GWs) optical counterparts (OTs). It can image simultaneously in three bands which cover u', Rc and Ic. To obtain the high atmospheric transmittance and image quality, the telescope was installed at the 5100m altitude site in Tibet Ali area. The construction of the entire telescope system has been finished recently. From the perspective of overview, this paper introduces optical layout, dome structure, and control technique. With the scientific data, we analyzed performances and parameters of the entire telescope system, including image quality, transmittance, and pointing errors. As one full robotic telescope, it will join the astronomy observation internationally in the future.

**Keywords:** Gravitational Waves, Optical Layout , CCD Camera, Transmissivity, Robotic Controlment.

*First Author, E-mail: liuwei@pmo.ac.cn

## 1 Introduction

The Gravitational Waves (GWs) are one of the direct predictions of general relativity. By detecting the gravitational waves of different wavelength band, GWs astronomy and quantum cosmic physics research will be promoted. GWs effect direction comes from dozens square degrees to 100 square degrees, and it is also difficult to identify whether the astrophysical phenomenon is the accompanying phenomenon of GWs or not. So it is necessary to observe the GWs events in large area with a wide range of bands, covering high-energy band to radio band. Besides LIGO/ Advanced and Virgo/ Advanced Virgo projects, Japan is developing the next gravitation wave telescope such as Kagra. Now the J-GEM (Japanese collaboration for Gravitational-wave

Electro-Magnetic follow-up) group has been established to explore the GWs phenomena. In optical band, we can analysis GWs effects by observing the fluctuation phenomenon of OTs and the electromagnetic waves from the central portion of the celestial body. In 2017, J-GEM has successfully observed the OT of the neutron star merger event GW170817 in optical and near-infrared bands[1]. Until now, many optical and infrared telescopes join the observation, like MITSuME 50cm, Akeno 50cm, Hiroshima University 1.5m Kanata, Kyoto University 3.8m Seimei, Subaru, Tyoko University TAO, Nagoya University MOA-II telescope, etc.[2] HinOTORI (Hirshima University Operated Tibet Optical Robotic Imager) is another new telescope which operates in optical band. The purpose of the telescope is to specialize in UV-optical follow-up observations of transient objects including OTs of gravitational wave (GW) sources, supernovae, GRBs, and so on in u', Rc and Ic band. It's observation capability, together with its special location will provide useful information for future GW events.

## 2 HinOTORI Telescope

### *2.1 Site*

HinOTORI telescope was installed at Ali observatory A point (Ali-A site) which locates at the ridge of a mountain with the high altitude about 5100 meters in Tibet Plateau of China. Ali observatory (32°31′373″N, 80°03′002″E), is an exceptional site with high atmospheric transmittance, shine percentage and low humidity which are suitable for observing cosmic microwave background radiation in the Northern Hemisphere. Figure1 indicates some climate parameters of Ali observatory.

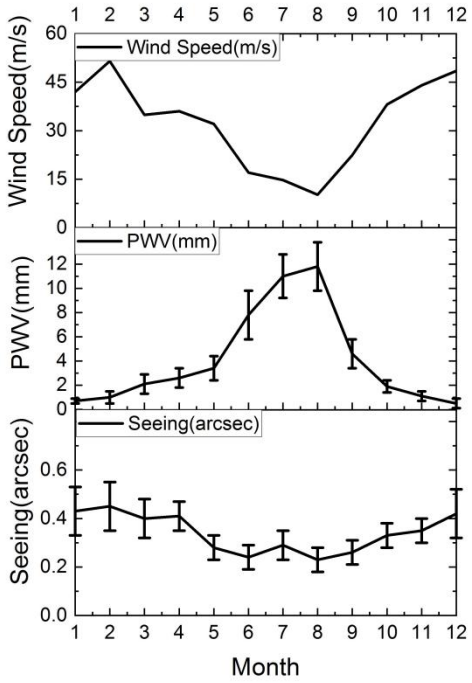


**Fig.1** Some climate parameters of Ali-A point. The wind speed means the monthly median wind speed in 2016 year at the height of the 200hPa pressure level. PWV (precipitable water vapor) was the quartile values in 2016, and it were integrated from 4280 m to 38 km above mean sea level from the statistics of all radiosonde data in each month. Seeing means the monthly seeing value at Beijing Time 07:00 in 2016 of 5050 m Ali-A site[3].

## *2.2 Telescope Instruments*

HinOTORI is a simultaneous muti-colour imaging telescope. The appearance is shown in Figure 2 and its basic parameters listed in Table1.

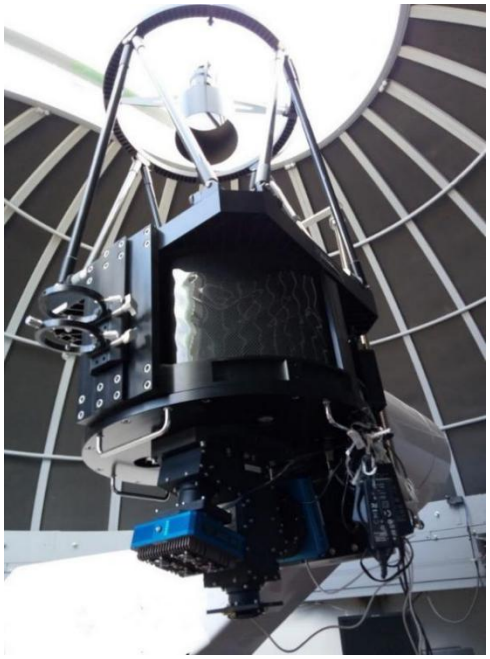

**Fig.2** HinOTORI telescope appearance

**Table1** The basic parameters of telescope

| Optical System | Ritchey-Chretien system |
|---|---|
| Diameter of the Primary Mirror | 510mm |
| Focal Length | 4080mm |
| Back focus | 460mm |
| Filter Band | u'(SDSS-u)/Rc/Ic |

Note: The central wavelength of u', Rc and Ic are 348.7nm, 656.4nm and 798.0 nm respectively.

Three CCD cameras were installed at each focal plane of 3 bands. The parameters of three cameras are listed in table2.

**Table 2** The Camera Parameters

| Parameters | u' Band | Rc Band | Ic Band |
|---|---|---|---|
| Sensor | E2VCCD42-40 | E2VCCD42-40 | E2VCCD42-40 |
| Resolution | 2Kx2K | 2Kx2K | 2Kx2K |
| Pixel Size | 13.5μm x13.5μm | 13.5μm x13.5μm | 13.5μm x13.5μm |
| Gain | 1.7(e-/count) | 1.3(e-/count) | 1.2(e-/count) |
| Field of View | 23'x23' | 23'x23' | 23'x23' |
| Readout Noise | 10.76e- | 9.14e- | 8.11e- |
| Dark Current (e-/pixel/sec) | 114.086@-24℃ | 0.15@-34℃ | 0.08@-36℃ |
| QE | 56%(350nm) | >90%(650nm) | 60%(800nm) |

Note: The details of E2VCCD42-40 sensor in u' Rc Ic bands are D02F-MG43D-U04240-UV1F, D09F-MG63D-U04240-MB0F and D09F-MG63D-U04240-MB0F respectively. In order to obtain high QE and observe in uv band, the camera window of u' band was made of UV-grade fused silica.

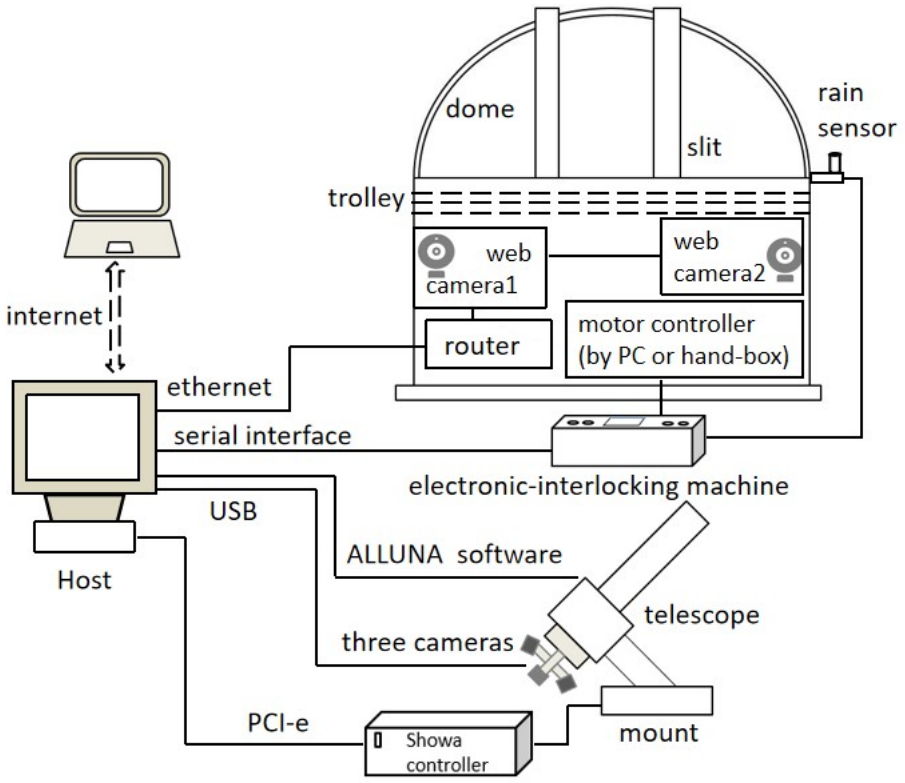


**Fig 3.** The Robotic system of HinOTORI

We have designed a robotic observation system as Figure 3 shows. The host controls almost all of the instruments, including mount, telescope, dome, three CCD cameras and web cameras. In basic layer, the mount, telescope and dome are controlled by ATLAS, TCS and ERDE respectively. We developed the overall software under Linux OS which integrates all the basic layer instruments. Synchronizer established the communication between host and dome rotation as well as slit motion. Now the CCD image data was saved to the local master computer. Typically, the raw observed data of three cameras is about 10GByte per night. We plan to build one NAS network storage server in the observatory and transfer large data to the telescope users. When we receive the gravitational wave (GW) event trigger or GRB alarm, we can operate the telescope for observation by remote control using desktop access solutions linked with Internet Network.

## 3 System Design

### *3.1 Optical Design*

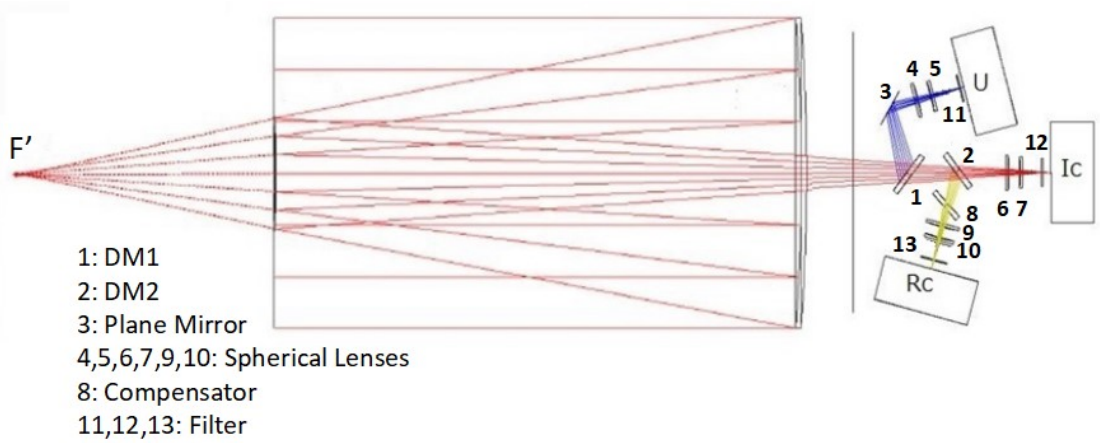


**Fig 4.** HinOTORI Optical Layout

HinOTORI is a typical Ritchey-Chretien long backfocus custom-made telescope. One of the reason for the long backfocus is to meet the space need of the simultaneous three band spectroscopic imaging. The optical layout is shown as Figure 4. In this optical system, the primary mirror and secondary mirror are designed as aspheric surfaces close to hyperboloid to correct coma and spherical aberration. Dichroic mirrors separate two bands by transmitting light of specific wavelength and reflect light of other wavelength. Two dichroic mirrors separate the main beam into u', Rc and Ic three channels. But these dichroic mirrors can lead optical path difference. Instead of using common correcting lenses, we designed the spherical correcting lenses system after dichroic mirrors. By adjusting the slope of the correcting lenses, the astigmatism, field curvature, and other optical abberations caused by the optical path difference can be eliminated.

To be specific, in the u' band, DM1 reflects the u' band light and one planar mirror and two correcting lenses and a filter are located behind it. In the Rc band, light after passing the DM1 is reflected by DM2. A wedged compensator glass and

correcting lenses were used to correct the astigmatic abberation. In the Ic band, light passes the DM1 and DM2, and after that we correct the light by inserting two spherical correcting lenses. Three filters were designed in front of the camera windows. As to the material, the filter was made of KG2, UG11 and fused silica in u' band, OG590 and synthetic quartz in Rc band, Rc-60 and HOYA colored glass in Ic band respectively. Two spherical lenses and CCD window are located at the back of the each light path. All the optical elements are coated with an AR coating to reduce reflection loss. The filters and dichroic mirrors were both made by Asahi Spectra company and the entire optical system was custom-made by OptCraft company according to the design.

*3.2 Telescope Control System*

The ToolKit and SDK of the instruments are developed and run under different OS. TCS software from Alluna, ATLAS software from Showa and Apogee CCD SDK are installed and run on Windows system. But the python program, IRAF and etc. run on Linux system. To meet the need of multiple OS, we adopted Vmware workstation as virtual machine in Windows OS, which supports Centos system. When integrating them into one system, the portability, maintainability and configurability should be considered. Taking these into consideration, we adopt ICE (Internet Communications Engine) as an object-oriented middleware, which supports Windows platforms as well as Linux platforms and manages communication among software processes. ICE has bindings for several programming languages, and it provides the possibility of easily creating objects that stand for the software tasks. The communication structure is shown as Figure 5.

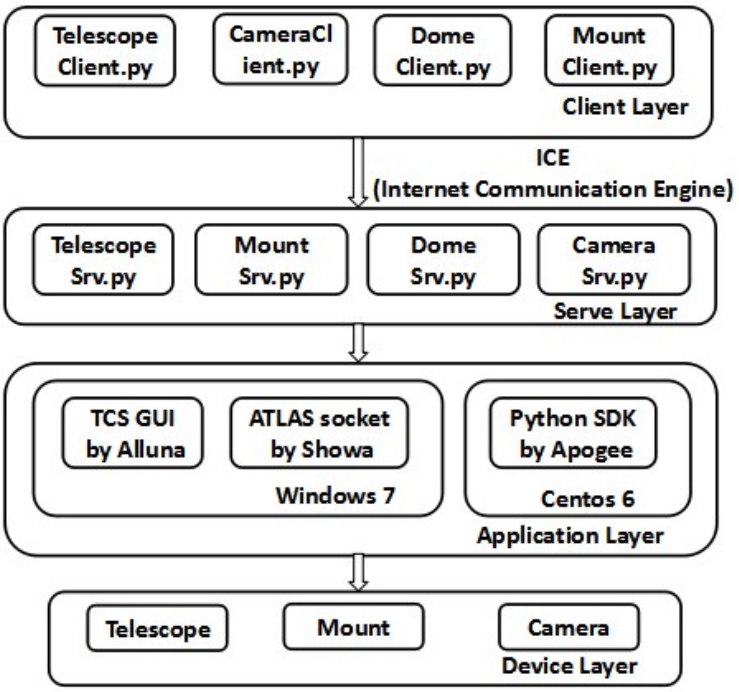


**Fig 5.** The communication structure based on ICE middleware

Actually, on the host side, Windows and Linux system have their dedicated IP respectively. HinOTORI.ice file is programmed as a module which define interfaces communication between Linux and Windows system. ICE package supports Python language,[4] and we use Python to program the server and client files. In client layer, we wrote telescope, mount, dome and camera python server programs, and they run independently.[5] In server layer, these four instrument server python files were programmed and run all the time. Once a server software receives commands from client programs through Ice, it executes the commands to trigger the functions in the application layer then control the actions of instruments in the device layer. The client programs are open for user to call on when programming in the upper layer.[6,7]

As a robotic telescope, the dome in this system can follow the position of the mount, act as a follow-up rotation with the mount pointing when working in automatical mode. The synchronizer takes charge of the communication between host and the dome motion. The control system structure diagram is shown as Figure 6.

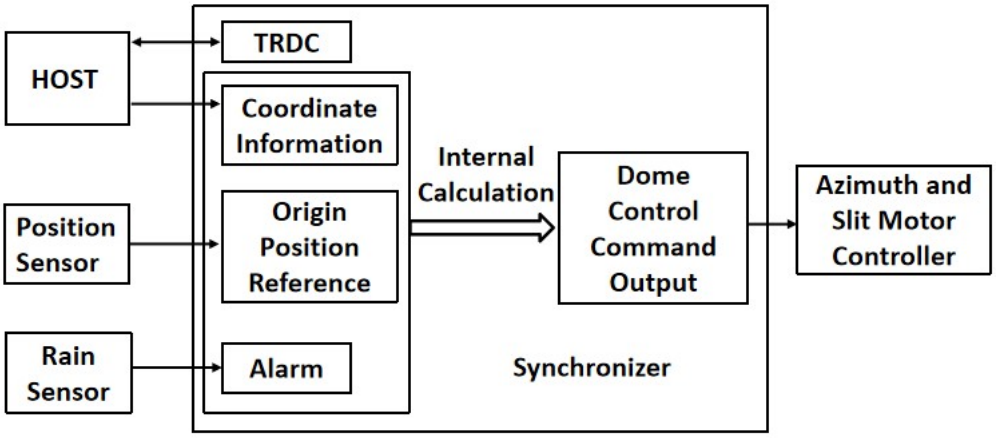


**Fig 6.** The structure diagram of the dome control system

A position switch was installed and looked as the dome origin position. After rotating the dome for one whole lap with the slit, synchronizer can remember the pluse counts of each positions. Knowing the origin point, calibrated one-lap pluse count, the synchronizer calculates the slit position independently when received the coordinate information from host. After the calculation finishes, the synchronizer send command to the motor controller and move the dome to the specific position that match with the position of the telescope pointing. All the motor operations can be achieved in automatic mode (TRDC software operation) or manual mode (hand-box operation), and they are independent from each other. If it rains during observation, under the monitoring of rain sensor and alarm connector to synchronizer, the dome will close automatically without human intervention.

## 4 Testing and Performances

### *4.1 Hartmann Analysis*

To evaluate the image quality and best focus position, we installed a Hartmann board with twenty holes in front of the second mirror. By adjusting the position of the second mirror through TCS software, we adjusted the focus from intra-focus to extra-focus step by step. In this process, we took images of three bands, and the

images comprised holes of the Hartmann board. After processing and analysis , we can obtain the size of aperture in images, which can be looked as Hartmann constant (HC). From the intra-focus to extra-focus process, aperture value follows the binomial distribution. Because the best focus leads to the minimum aperture value, , the best focus position can be located by calculating the minimum aperture value. In the observation of 2018 October, the results are listed as table3.

**Table 3** Best Focus and Corresponding Hartmann Constant

| Filter | Date | Best Focus[mm] | HC [arcsec] |
|---|---|---|---|
| Rc | 2018/10/15 | 3.90 | 0.61±0.06 |
| Ic | 2018/10/15 | 3.89 | 0.63±0.06 |
| U’ | 2018/10/18 | 3.95 | 0.49±0.06 |
| Rc | 2018/10/18 | 3.96 | 0.56±0.07 |
| Ic | 2018/10/18 | 3.95 | 0.60±0.07 |

In 2015 January, before installed in China Tibet Ali site, the entire system was tested in Hiroshima, Japan. At that time, the HC values of Rc and Ic bands were 0.60±0.05 and 0.59±0.05 respectively. Comparing these two data, we think the optical system had rarely changed. In addition, the best focus has correlation with the environment temperature, and it can contribute to certain focus variation. The best focus position should be adjusted under different environment in different seasons.[8]

*4.2 Image Quality*

With this best focus and 60 seconds exposure time, we took the images of the Z_And area (ra,dec)=(340.560,48.615) in three bands. In this area, we can observe many bright star. There are about two hundreds stars with magnitude brighter than 10 mag in u’ Rc and Ic band. To evaluating the image quality, we calculated the full width of half maximum (FWHM) of the point spread function (PSF) using the Z_And images

in three bands. The FHWM distribution diagram of three bands are shown as Figure 7,8, and 9.

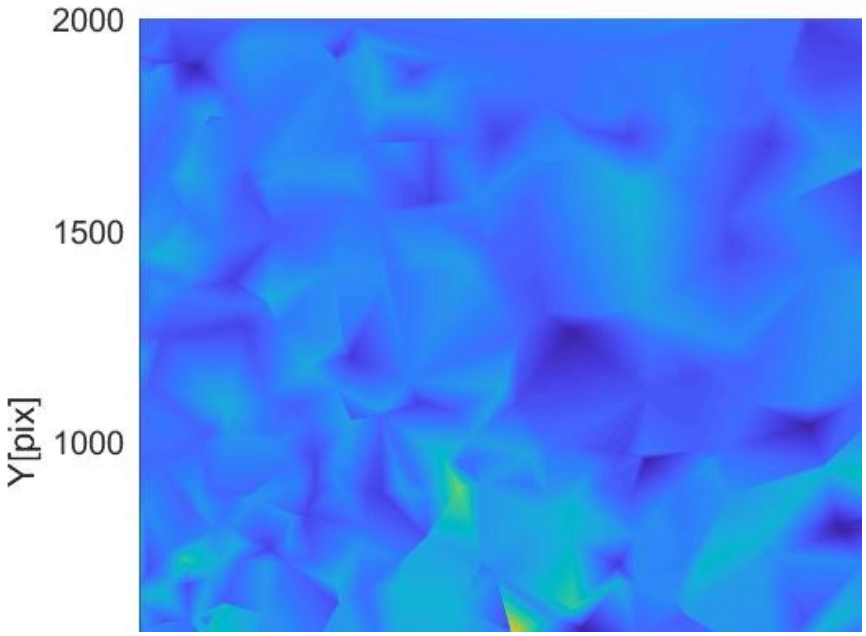


**Fig7.** FWHM distribution diagram of U' band image

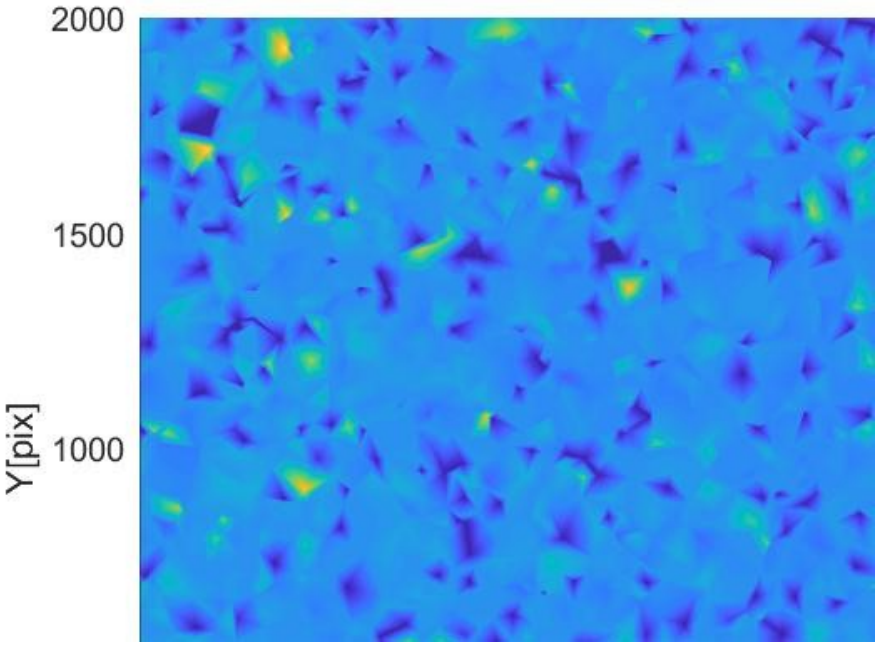


**Fig8.** FWHM distribution diagram of Rc band image

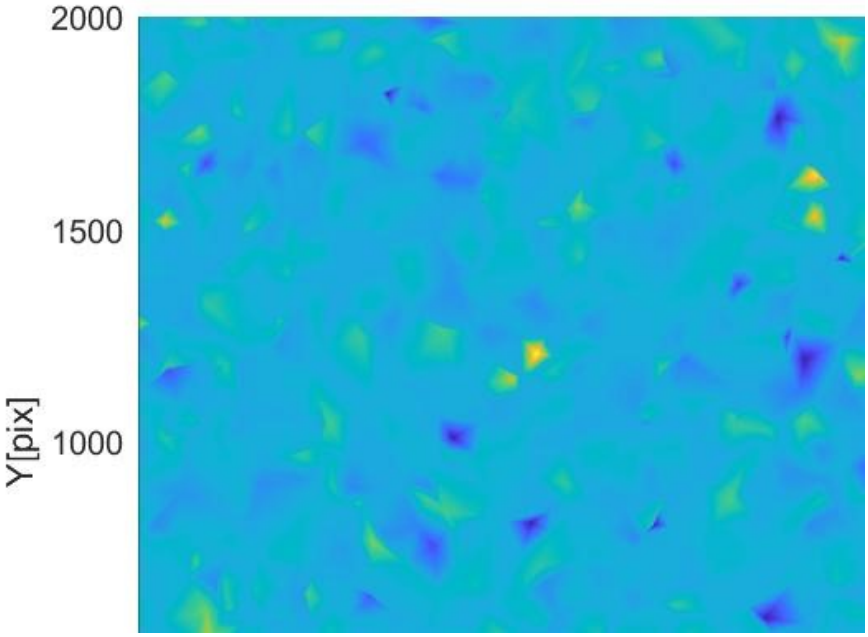


**Fig 9.** FWHM distribution diagram of Ic band image

The average value of FWHM in u', Rc and Ic bands are 4.66, 3.93, and 3.83 pixel, and the standard deviations are 2.04,1.62, and 0.81 respectively. The FWHM distribution diagrams indicate that FWHM follow uniform distribution in general. From these value, we think that the three positions of CCD photosensitive areas and focus are in the good condition. It is possible to use the images to process astronomical analysis.

*4.3 Pointing Error*

We use several stars to calibrate the polar axis alignment. The declinations covered from 0° to 36° in the stellar field. From the star offset position in the fits file, we adjusted elevation and azimuth degree of the telescope. By calculating the CRVAL, CRPIX, and CDELT value in the fits file information, which means the coordinate at the reference pixel, the value of the reference pixel, and the increment between pixels, respectively, the center position of equatorial coordinate can be attained. The formulas are listed as follows:

Center RA= CRVAL1 + CDELT1 * ( 1024 - CRPIX1 ) (1)

Center Dec= CRVAL2 + CDELT2 * ( 1024 - CRPIX2 ) (2)

As to the HinOTORI system: CDELT1=CDELT1=0.000187degrees/pixel. Compared with the value input to the telescope driver, we checked the pointing error using TheSky assistant software which indicated that pointing error was one arcmin, even though this value depends on the quality of the image. Also some other factors may affect the result, such as gravitational deformation, airmass, and the mechanical drive system of equatorial mount. We think this pointing performance is acceptable.

*4.4 Limiting Magnitude*

The Standard magnitude M and telescope observed flux follow the formula that :

M =-2.5log10Flux+zp, where zp is the zero-point, which is a comprehensive parameter including the effects of instrument, telescope transmittances, airmass and detector electronics. To calculate zp, several Landolt photometric standards star, including SA92-276, SA97-75, SA92-282 were selected as objects for calculation. We looked up the magnitudes of these stars on the star catalogue of each band. After bias substraction, flat fielding preprocession and WCS (World Coordinates System) calibration, we extracted the flux information and zero-point according to these fluxes of stars.

The results are listed as Figure10. The zero-point value has the positive correlation with exposure times, which means increasing exposure time is helpful to capture the fainter objects. When the exposure time is 60 seconds, the zero-points are 23.163, 26.287 and 25.385 for u’ Rc and Ic bands.

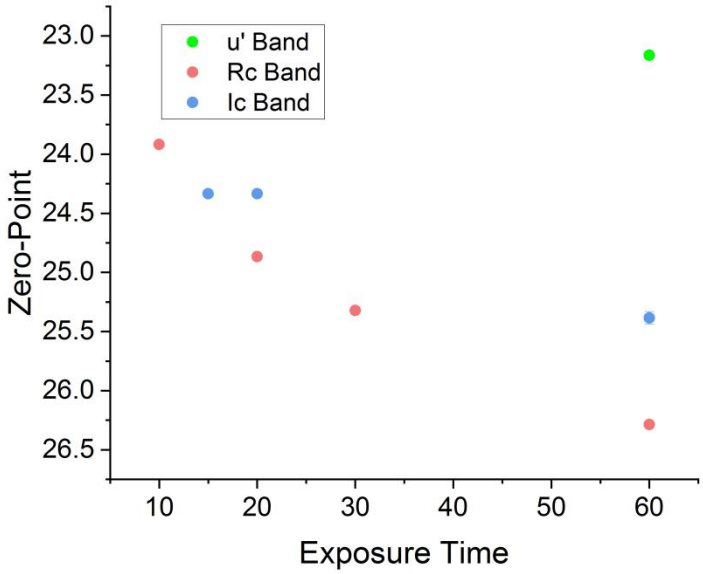


**Fig.10** Zero-Point calculation of 3 bands

With the magnitude zero-points, the formulas of different bands can be written as follows.

$$mag\_u' = -2.5 \lg(flux) + 23.163 \quad (3)$$

$$mag\_Rc = -2.5 \lg(flux) + 26.287 \quad (4)$$

$$mag\_Ic = -2.5 \lg(flux) + 25.385 \quad (5)$$

Set the photometry aperture at 3 FWHM, we obtain the limiting magnitude of three bands. As in the context of figure 11, the 10σ limiting magnitudes in u', Rc and Ic bands are 13.511, 17.898 and 17.335 mag respectively with 60s exposure time.[9]

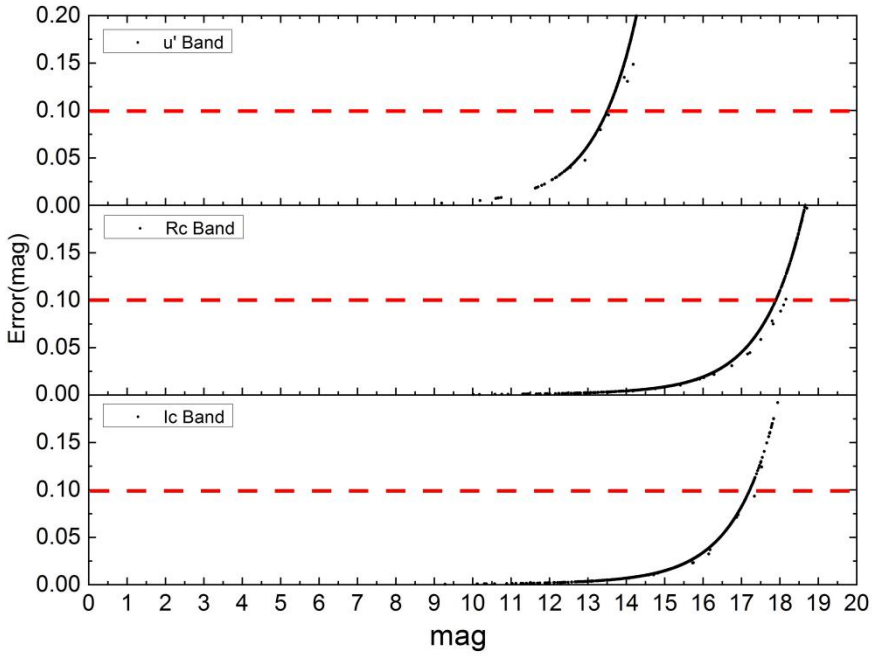


**Fig 11.** u' Rc and Ic magnitudes versus magnitude errors of the Rubin149 area with 60s exposure time.

### *4.5 Total Transmittance*

Many factors contribute the total transmittance. In optical instrument perspective, the main factors include the transmittance of three bands' filters, dichroic mirrors (DM1 and DM2) and lenses as well as the CCD QE factor. Another important factor is the atmosphere optical extinction. Referring to the MODTRAN software which adopted 1976.US standard atmosphere data,[10] we simulated the atmospheric transmittance of Ali-A site of 5100m altitude, and used it as the atmosphere factor. Combining this atmosphere factor with the other factors, we simulated the total transmittance for the three bands, which are shown in Figure 12.[11]

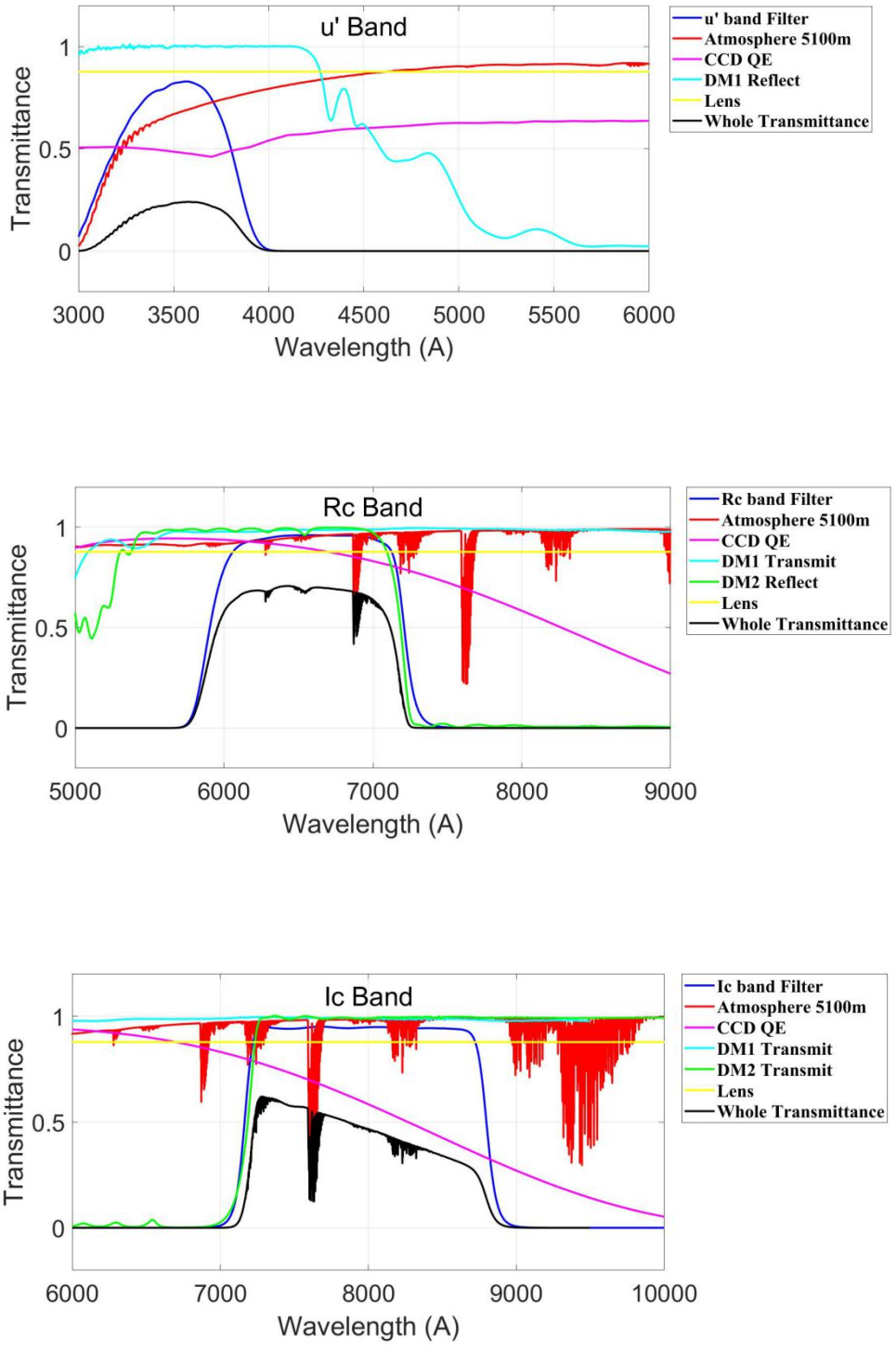


**Fig 12.** Total efficiency in three bands

Rc band presents the highest efficiency. As for u' band, the atmosphere transmittance and CCD QE play major role in the efficiency reduction. The short wavelength light from astronomical sources, with the effect of Rayleigh scattering, have the relative lower transmittance compared to the long wavelength. Specifically,

ultraviolet cutoff is due to the high altitude selective molecular bands of the ozone layer. While for Ic band, the atmosphere transmittance improves a lot, and the extinction at long wavelengths is mainly due to bigger particles (dust and aerosols), and the main factor of efficiency loss attributes to the low CCD QE performance.

## 5 Summary and future work

In this paper we introduced the overview of HinOTORI telescope, mainly focused on the overall structure, three-band optical design, CCD camera performances, multi-device automatic control method based on ICE communication, dome rotation control, and the basic characterization of the telescope. Now the entire telescope and dome system have been built up, and we can use it to observe on site or through remote control by network. The observation system now is in the debugging stage, and more accurate parameters will be measured soon afterwards.

Together with Advanced LIGO and advanced Virgo observing run, as a part of J-GEM, HinOTORI will join the observation of OTs triggered by GWs events. Compared to some other telescopes, HinOTORI has its own advantages including high atmospheric transmittance in high altitude and three band simultaneous imaging, highly-automated operation, etc. These advantages will also be conducive to observe not only GWs, but the gamma burst, supernova stars and other variable star as well.

***Acknowledgments***

We are grateful for the assistance of many persons during the construction and instruments commissioning. The staff from National Astronomical Observatories of China gave huge support during the entireconstruction. We would like to thank Kuroshima who helped us to build the dome on site and gave advice about the dome robotic control design. Showa mount company also gave valuable instructions during

adjusting the alignment of polar axis.

## *References*


1. Yousuke Utsumi, et al., J-GEM observations of an electromagnetic counterpart to the neutron star merger GW170817, PASJ, 69, 6 (2017)

2. Yatsu Yoichi, et al., Development of MITSuME—Multicolor imaging telescopes for survey and monstrous explosions, Physica E, 40, 2 (2007)

3. Xuan Qian, et al. The Characteristics at the Ali Observatory Based on Radiosonde Observations, Publications of the Astronomical Society of the Pacific, 130, 994 (2018)

4. Weiner Benjamin J. et al., Development of the Arizona Robotic Telescope Network,SPIE, 10704 (2018)

5. Frank Kittmann, et al., Design and implementation of a service-oriented driver architecture for LINC-NIRVANA , SPIE, 7019 (2008)

6. Juergen Berwein, et al., An SOA developer framework for astronomical instrument control software, SPIE, 7019 (2008)

7. Yousuke Utsumi, et al., Hyper Suprime-Cam: the Control System, SPIE, 8446 (2012 )

8. Nobunari Kashikawa, et al., FOCAS: The Faint Object Camera and Spectrograph for the Subaru Telescope, PASJ, 54, 6 (2002)

9. T. Baug, et al., TIFR Near Infrared Imaging Camera-II on the 3.6 m Devasthal Optical Telescope, Journal of Astronomical Instrumentation, 7, 1 (2018)

10. J.S. Lawrence. Infrared and Submillimeter Atmospheric Characteristics of High Antarctic Plateau Sites, Publications of the Astronomical Society of the Pacific, 116(2004)

11. Chung Haeun, et al., DOTIFS a new multi-IFU optical spectrograph for the 3.6-m Devasthal optical telescope, SPIE, 9147 (2014)